Breast cancer cells promote osteoclast differentiation in an MRTF-dependent paracrine manner

Pooja Chawla[1], David Gau[1], Fangyuan Chen[2,3], Niharika Welling[4], David Boone[5], Juan Taboas[1,6], Adrian V. Lee[7], Deborah L. Galson[8], Partha Roy[1,9]

[1]Bioengineering, University of Pittsburgh
[2]School of Medicine, University of Pittsburgh
[3]School of Medicine, Tsinghua University, China
[4]Computational and Systems Biology, University of Pittsburgh
[5]Biomedical Informatics, University of Pittsburgh
[6]School of Dentistry, University of Pittsburgh
[7]Pharmacology, University of Pittsburgh
[8]Hematology-Oncology Department of Medicine, University of Pittsburgh
[9]Pathology, University of Pittsburgh

Corresponding author:
Partha Roy, Ph.D, 306 CNBIO, 300 Technology Drive, University of Pittsburgh, Pittsburgh, PA 15219, USA; Tel: 1-412-624-7867; Fax: 412-383-8788; Email: par19@pitt.edu

Running title: Role of MRTF in osteoclastogenesis

ABSTRACT

Bone is a frequent site for breast cancer metastasis. Conditioning of the local tumor microenvironment (TME) through crosstalk between tumor cells and bone resident cells in the metastatic niche is a major driving force for bone colonization of breast cancer cells. The vast majority of breast cancer-associated metastasis is osteolytic in nature, and RANKL-induced differentiation of bone marrow-derived macrophages to osteoclasts (OCLs) is a key requirement for osteolytic metastatic growth of cancer cells. In this study, we demonstrate that breast cancer cell-secreted factors stimulate RANKL-induced OCL differentiation of BMDMs requiring the function of Myocardin-related transcription factor (MRTF) in tumor cells. This is partly attributed to MRTF's critical role in maintaining the basal cellular expression of connective tissue growth factor (CTGF), a pro-osteoclastogenic matricellular factor known to promote bone metastasis in human breast cancer. Supporting these *in vitro* findings, bioinformatics analyses of multiple human breast cancer transcriptome datasets reveal a strong positive correlation between CTGF expression and MRTF gene signature further establishing the relevance of our findings in a human disease context. By Luminex analyses, we show that MRTF depletion in breast cancer cells has a broad impact on OCL-regulatory cell-secreted factors that extends beyond CTGF. These findings, taken together with demonstration of MRTF-dependence for bone colonization breast cancer cells *in vivo*, suggest that MRTF inhibition could be an effective strategy to diminish OCL formation and skeletal involvement in breast cancer. In summary, this study highlights a novel tumor-extrinsic function of MRTF relevant to breast cancer metastasis.
Keywords: MRTF, SRF, bone, metastasis, osteoclast, CTGF

INTRODUCTION

Breast cancer is one of the leading causes of cancer-related death in women. The vast majority of breast cancer-related deaths are due to the metastatic spread of tumor cells to distant organs. Bone is a frequent site of breast cancer metastasis with the median survival of patients after tumor cells have metastasized to the bone being 2-3 years (1-4). Bone metastasis falls into three different categories, namely osteolytic (involves bone resorption), osteoblastic (involves deposition of new bone), and mixed (involves both formation and resorption of bone) with the vast majority of breast cancer-associated metastasis being osteolytic in nature (>70%) (5). Metastasis to the bone is complex process that involves chemotactic migration and attachment of circulating tumor cells to the bone surface, and subsequent interactions between cancer cells and various stromal cells in the bone microenvironment that lead to a vicious cycle of bone remodeling. Under normal conditions, bone-forming osteoblasts (OBs) produce macrophage colony-stimulating factor (MCSF) and receptor activator for nuclear factor κB (NFκB) ligand (RANKL) which stimulate proliferation and differentiation of myeloid progenitor cells from the bone marrow into macrophage/monocyte lineage cells and their subsequent differentiation/maturation into osteoclasts (OCLs), a type of cells that is responsible for degradation of mineralized bone. However, OBs also produce osteoprotegerin (OPG) which binds to and sequesters RANKL thereby limiting OCL activity and regulating the levels of bone resorption (6-9). The balancing act of OBs and OCLs is dysregulated in the presence of tumor cells where osteoclastogenesis and OCL survival are greatly enhanced by increased secreted levels of RANKL and other soluble factors (e.g. IL6, IL11, IL1, TNF, PTHrP) contributed by tumor cells, osteocytes, OBs and immune cells (10-12). Increased bone resorption promotes the release and activation of ECM-bound growth factors and cytokines, further amplifying this loop and stimulating tumor cell proliferation and metastatic colonization of tumor cells (13).

Myocardin-related transcription factors (MRTFs) are key coactivators of serum-response factor (SRF) that link actin dynamics to SRF-mediated transcription of a wide variety of genes including SRF itself and many others which play important roles cytoskeleton remodeling, cell adhesion and ECM regulation (14-16). There are two major isoforms of MRTF, namely MRTF-A (also known as MKL1 or BSAC) and MRTF-B (also known as MKL2). Both MRTF isoforms are ubiquitously expressed, share structural and functional similarities, and compensate for each other in most loss-of-function settings. However, phenotypic differences between mice deficient in MRTF-A vs-B suggest that these isoforms are not completely functionally redundant (17, 18).

Consistent with the role of the MRTF/SRF transcriptional axis in regulating the expression of many structural and regulatory components of actin cytoskeleton, depletion of either MRTFs or SRF causes defects in actin cytoskeleton and cell migration of both normal and cancer cells (including breast cancer cells) *in vitro* and *in vivo* (comprehensively reviewed in (16)). Silencing the expression of either MRTF or SRF also dramatically impairs experimental lung colonization ability of breast cancer and melanoma cells *in vivo* (19). Supporting these findings, we recently demonstrated that MRTF-depletion induces an outgrowth-arrest phenotype in breast cancer cells, and conversely, overexpression of either MRTF-A or MRTF-B accelerates initiation and progression of breast cancer cells on soft ECM substrate. Our *in vivo* studies further showed that SRF's interaction with MRTF is critical for the intrinsic tumor-initiating ability and post-extravasation metastatic outgrowth of breast cancer cells in immunodeficient mice (20). Interestingly, when MRTF is overexpressed in breast cancer cells, increased actin polymerization and cell stiffening also increases susceptibility of tumor cells to cytotoxic T cell attack thereby limiting lung colonization of tumor cells through immune surveillance (21). Collectively, these findings suggest that a balanced MRTF activity in tumor cells is perhaps most efficient for their metastatic colonization ability in the presence of a functional immune system.

MRTF's role in metastatic colonization of cancer cells has been primarily investigated in the context of soft organs to date, and those studies focused exclusively on tumor-intrinsic impact of perturbation of MRTF. Bone represents a unique structural organ in terms of its physiochemical characteristics (ECM composition and stiffness) and parenchymal/non-parenchymal cellular compositions. The objective of the present study was to investigate tumor-extrinsic impact of perturbation of MRTF, specifically examining its potential role in tumor-cell directed paracrine modulation of OCL differentiation.

RESULTS

MRTF plays a critical role in tumor cell-directed modulation of osteoclast differentiation

Since loss-of-expression of one isoform of MRTF can be functionally compensated by the other isoform, to investigate MRTF's potential role in tumor-cell directed paracrine modulation of OCL differentiation, we genetically engineered GFP/luciferase-expressing sublines of MDA-MB-231 (MDA-231 – a human triple-negative breast cancer [TNBC] cell line) and D2.A1 (a murine TNBC cell line) for shRNA-mediated stable co-suppression of MRTF isoforms. Corresponding non-targeting control shRNA-transfectants served as controls. Depending on the cell line and the isoform of MRTF, we achieved an average of 60-90% reduction of MRTF isoforms at the protein level in the MRTF-A/B shRNA (referred to as MRTF-knockdown hereon) sublines vs their respective controls (**Figs 1A-B**). Reduction of the total MRTF level

diminished the rate of proliferation of both breast cancer cell lines in 2D culture, although the effect was more prominent in D2.A1 cells likely due to better knockdown efficiency (**Fig 1C**). For OCL differentiation studies, we first differentiated bone marrow progenitor cells harvested from female FVB mice into macrophages (denoted as bone marrow-derived macrophages or BMDMs in short) by MCSF (macrophage colony stimulating factor) treatment. Subsequently, we differentiated BMDMs into OCLs by co-treatment of RANKL and MCSF with or without supplementation of conditioned media (CM) harvested from 2D cultures of control vs stable MRTF knockdown breast cancer (MDA-231 and D2A1) cells (the experimental schematic is shown in **Fig 2A**). BMDMs without RANKL exposure served as the control group in these experiments. Although stable knockdown of MRTF reduced proliferation of both breast cancer cell lines in 2D culture, the total protein concentration in the CM was not significantly affected by reduced MRTF expression in either of the two cell lines (**supplementary Fig S1**). Induction of expression of Tartrate-resistant alkaline phosphatase (TRAP - encoded by the *ACP5* gene), an enzyme involved in hydrolysis of bone matrix, is a hallmark of OCL differentiation, and the phosphatase activity of TRAP (a proxy marker of osteoclastic bone resorption (22)) can be visualized in cells by a well-established colorimetric assay (23). Therefore, we performed end-point colorimetric TRAP activity staining of cultures to identify and score mature OCLs which were characterized by TRAP-staining-positive multi-nucleated (presence of 3 or more nuclei) cells (representative images of TRAP-stained cells from these experiments are shown in **Fig 2B)**. In general, the total cell counts of CM-exposed BMDM cultures were lower than those without although MRTF-depletion in tumor cells per se did not have any effect on the total cell counts of BMDM cultures (**Fig 2C**). Because of the differences in the total cell counts of BMDM cultures between the groups, we quantified mature OCL count as a % of total number of cells in the culture as a measure of OCL differentiation efficiency and normalized to the same calculated for RANKL-alone treatment group (termed as "OCL differentiation index") for comparison between different groups. In both cell line experiments, RANKL addition dramatically promoted OCL differentiation of BMDMs as expected. RANKL-induced OCL differentiation index was further enhanced when BMDMs were exposed to the CM harvested from control shRNA cells, and this trend was not only reversed but was also actively repressed when MRTF expression was stably silenced in breast cancer cells (**Fig 2D**). DC-Stamp (dendritic cell-specific transcription protein - a transmembrane protein) and Cathepsin-K (a protease) are major regulators of osteoclastogenesis, and deficiency of either is linked to decreased differentiation and/or activity of OCLs (24, 25). Specifically, DC-stamp is responsible for cell-cell fusion giving rise to the multinucleated mature OCL phenotype (25). Cathepsin-K plays a key role in proteolytic cleavage and conversion of the inactive TRAP precursor protein (the initially synthesized form) into an active form (26). Consistent with our OCL differentiation readout data, quantitative RT-PCR analyses showed that RANKL-induced expressions of both DC-stamp and Cathepsin-K in BMDMs are further enhanced by MDA-231 secreted factors in an MRTF-dependent manner (**Fig 2E**). As an additional validation, we also repeated these OCL differentiation studies in a transient knockdown setting of MRTF isoforms in MDA-231 cells. For these studies, we combined siRNAs targeting regions of MRTF-A and MRTF-B mRNAs that are different from the common region targeted by the shRNA for stable knockdown. Although exposure to CM harvested from siRNA-transfected tumor cells did not reduce the proliferation of BMDM cultures as we observed in the case of stable knockdown setting, the overall trend of tumor cell-derived factors promoting RANKL-induced OCL differentiation in an MRTF-dependent manner was also recapitulated in the transient knockdown setting (**supplementary Fig S2**). Overall, these findings are consistent with a scenario that that breast cancer cells stimulate RANKL-induced OCL differentiation of BMDMs in an MRTF-dependent paracrine signaling manner.

As a complementary set of experiments, we also investigated the effect of overexpression of either wild-type (WT) MRTF-A or select functional mutants of MRTF-A on tumor cell-directed paracrine regulation of OCL differentiation. Although SRF-activation is the most well-studied function MRTF, both MRTF isoforms contain a SAP (SAF-A/B, Acinus and PIAS – named after the proteins the domain was originally discovered in) domain commonly found in other DNA-binding proteins. At least in a transient transfection setting, deletion of the SAP domain does not affect MRTF's ability to activate SRF (27). However, overexpression of SAP-domain-deficient mutant form of MRTF-A induces transcriptomic changes in cells that are distinct from those elicited by overexpression of K237A/Y238A/H239A/Y241A-MRTF-A (an SRF-binding deficient mutant of MRTF-A) which led to a postulate that MRTF may also activate gene transcription directly utilizing its SAP domain in an SRF-independent manner (28-30). We previously engineered GFP/luciferase expressing sublines of MDA-231 cells for doxycycline-inducible overexpression of either wild-type form of MRTF-A (WT-MRTF-A) or K237A/Y238A/H239A/Y241A-MRTF-A (denoted as ΔSRF-MRTF-A) or SAP-domain-deleted mutant of MRTF-A (denoted as ΔSAP-MRTF-A), and demonstrated that overexpression of ΔSRF-MRTF-A specifically blocks the intrinsic tumor-initiating ability and post-extravasation metastatic outgrowth of breast cancer cells (20). For the present study, we utilized those sublines of MDA-231 cells to determine whether CM derived from these various MRTF-A overexpressing sublines has any differential effect on RANKL-induced OCL differentiation. Although overexpression of WT-MRTF-A did not further potentiate OCL differentiation when compared to control, CM derived from either ΔSRF- or ΔSAP-MRTF-A overexpressing sublines actively repressed OCL differentiation mimicking the knockdown experimental results (**Fig 3**). Note that the total cell count of BMDM culture was not significantly different between experimental conditions that involved treatment of CM derived from any of the MRTF-A overexpression cultures. These data further suggest that both SAP-domain- and SRF-related activities of MRTF are important for tumor-cell directed paracrine regulation of OCL differentiation.

MRTF depletion in breast cancer cells downregulates multiple pro-osteoclastogenic cell secreted factors. To gain insight into how loss of MRTF expression in breast cancer cells dampens RANKL-induced OCL differentiation in a paracrine manner, we first compiled a signature of 21 genes based on two previously published findings (12, 31) that are associated with bone metastasis in human breast cancer (**supplementary Table S1**). We then queried this gene set against previously published differentially expressed genes (DEGs) of 2D cultures of MDA-231 cells upon stable co-silencing of MRTF isoforms (19). Based on this query, we identified three bone metastasis-associated genes that are downregulated in mRNA expression upon MRTF silencing, including CTGF/CCN2 (consistent with a previous finding in endothelial cells in an overexpression setting (32)), IL11, and FGF5. From our unpublished RNA-seq analyses of 2D and 3D cultures of GFP/Luc expressing sublines of MDA-231 cells with or without overexpression of WT- vs functional mutants of MRTF-A (GSE253047), we were able to further verify that expressions of all three genes are increased in MDA-231 cells when WT MRTF-A is overexpressed (**Fig 4A**) although the effect of functional disruption of MRTF on its ability to induce these genes was found to be gene-specific. While MRTF-A's ability to induce CTGF expression at the transcript level requires both SRF- and SAP-domain-related functions, induction of IL11 and FGF5 were selectively dependent on SRF- and SAP-domain-related functions of MRTF-A, respectively. In general, there was good concordance in the patterns of expression of these three genes between the 2D and the 3D culture conditions.

Interestingly, all three genes (CTGF, IL11 and FGF5) encode for cell-secreted factors that are known to promote OCL differentiation and/or activity (33-35). However, when we analyzed three large human breast cancer transcriptome databases (METABRIC [n=1981] (36), TCGA [n=1208] (37), and SCANB [n=3207] (38); n represents the number of clinical samples), only CTGF expression showed a strong positive correlation (spearman's correlation coefficient >0.6) with the MRTF gene signature score (constructed based on GSVA analyses (39)) in primary tumors consistently in all three transcriptome databases (**Fig 4B**). Furthermore, between the two isoforms, expression of only MRTF-A has a significant positive association with CTGF expression in human breast cancer (**Fig 4C**). Based on these clinical correlation findings, we chose to further interrogate CTGF as a candidate mediator of MRTF-dependent paracrine regulation of OCL differentiation.

Although overexpression studies demonstrate MRTF-A dependent stimulation of CTGF expression (32), given that CTGF expression can be also regulated by other transcription factors (e.g. YAP (40)), to what extent MRTF is required for maintaining the basal CTGF expression at the protein level is not known. We found that MRTF knockdown in both MDA-231 and D2A1 cells results in a dramatic reduction (~80-90% depending on the cell line) in CTGF expression at the protein level, suggesting that MRTF is absolutely essential for maintaining the basal expression of CTGF (**Fig 5A-B**). We also compared the CTGF expression between the various MRTF-A overexpressing sublines of MDA-231 cells relative to the control subline, the results of which are shown in **Fig 5C**. Consistent with the knockdown experimental results, overexpression of WT-MRTF-A increased CTGF expression relative to control in all three independent experiments with the p-value (=0.07) close to statistical significance (note that the variation in the fold-change accounts for the p-value not reaching statistical significance). MRTF-A-induced increase in CTGF expression was completely reversed upon functional disruption of either SRF's interaction or SAP-domain function. CTGF expression in ΔSRF-MRTF-A expressers was the least among all four groups indicating a critical importance of SRF's interaction of MRTF is maintaining the basal cellular CTGF expression.

Next, we asked whether CTGF supplementation can rescue OCL differentiation defect of BMDMs in the setting of MRTF knockdown setting. Previous studies reported CTGF supplementation at 50-100 ng/ml boosts RANKL-induced OCL differentiation in BMDMs (derived from IJR strain male mouse) and RAW264.7 (a Balb/c mouse-derived tumorigenic macrophage cell line) cells (33, 41). In a rescue setting, CTGF addition at 50 ng/ml concentration reversed the dampening of RANKL-induced OCL differentiation of BMDMs induced by CM of MRTF-silenced MDA-231 cells (note that the total cell count in the BMDM culture was not impacted by CTGF addition) (**Figs 5D-E)**. Increasing CTGF concentration from 50 to 100 ng/ml did not result in any further increase in OCL differentiation in the BMDM culture. These data suggest that CTGF is an important paracrine mediator of pro-osteoclastogenic action of MRTF in breast cancer cells.

Since CTGF supplementation was not sufficient to abrogate the difference in the OCL differentiation index of BMDMs between the two (i.e. control vs MRTF-knockdown) CM exposure settings (**Figs 5D-E**), we postulated that MRTF depletion in breast cancer cells may alter secretion of additional pro- and/or anti-osteoclastogenic factors. Many immunomodulatory cytokines and chemokines play a prominent role in both positively and negatively regulating proliferation, survival and differentiation of OCL (42). Therefore, we performed Luminex analyses of CM harvested from control vs MRTF knockdown cultures of MDA-231 cells and D2A1 cells to profile a panel of 48 human and 32 mouse cytokines/chemokines, respectively

(**supplementary Table S2** lists the cytokines/chemokines probed by each of these multiplexed Luminex panels with the common ones indicated by red). We detected a total of 13 differentially abundant factors (within statistical significance) between the two groups with 7 factors upregulated (IL1RA, IP10/CXCL10, IL1β, TGFα, fractalkine/CX3CL1, IL27, RANTES/CCL5) and 6 factors downregulated (IL8, G-CSF, FGF2, IL3, IL17E/IL25, FLT3L) in the CM of MDA-231 cells upon MRTF knockdown within statistical significance (**Fig 6A**). Among these factors, upregulation of anti-osteoclastogenic factors (IL1RA and IL27) and conversely, downregulation of pro-osteoclastogenic factors (IL8, G-CSF, and FLT3L) are consistent with repression of OCL differentiation in an MRTF knockdown setting. Similarly, analyses of D2.A1 CM revealed a total of 10 differentially abundant factors between the two groups with 1 factor upregulated (IL7) and 9 factors downregulated (MIP1a/CCL3, LIX/CXCL5, GM-CSF, MCP1/CCL2, Eotaxin, IL1α, IL6, G-CSF) upon MRTF knockdown within statistical significance (**Fig 6B**). Among these factors, reduction in G-CSF, CCL2, CCL3, IL1α, IL6 and Eotaxin are directionally consistent with repression of OCL differentiation in the MRTF knockdown setting. Collectively, these data demonstrate that loss of MRTF expression in breast cancer cells has a broad impact on the secretion of OCL-regulatory factors. The general lack of consensus in differentially abundant cytokines/chemokines between these two sets of Luminex data was not surprising because of inherent differences between human vs mouse breast cancer cell lines. However, reduced secreted level of G-CSF and potential downregulation of IL1 signaling (as suggested by reduction of secreted IL1 or upregulation of secreted IL1 receptor antagonist [IL1RA]) upon MRTF depletion seemed to be a common feature in both breast cancer cell lines. It is worth noting that we did not find evidence for changes in the mRNA levels of any of these immunoregulatory factors when we queried previously published microarray data (19) and our own RNA-seq data of MDA-231 cells in knockdown and overexpression settings of MRTF, respectively. This suggests that MRTF-dependent changes in these immunomodulatory factors are most likely not through direct transcriptional control.

MRTF depletion inhibits experimental bone colonization of breast cancer cells

To query MRTF's role in bone colonization of breast cancer cells, we first performed intracardiac injection-based experimental metastasis assays with control *vs* MRTF knockdown MDA-231 cells in immunodeficient NOD-SCID-gamma (NSG) mice. Although orthotopic models represent the entire cascade of events of metastasis, we chose experimental metastasis assays to exclusively assess the impact of loss of MRTF expression on metastatic growth of breast cancer cells in bone without confounding effects of MRTF-dependent changes in primary tumor growth and/or tumor cell dissemination. Intracardiac experimental metastasis assay allows for widespread metastasis of cancer cells including to the bone. Use of NSG mice also enabled us to decouple the secondary effect of MRTF on immune surveillance in metastatic colonization process. Bioluminescence imaging (BLI) revealed that 6 out 8 animals (75%) animals inoculated with control MDA-231 subline exhibited skeletal metastasis in the long bones within 11 days after injection, compared to only 1 out 8 (12.5%) animals injected with MRTF knockdown cells presenting the same (**Fig 7A;** BLI quantification and skeletal metastasis confirmation by bone histology are shown in **7B-C**). Although the intracardiac injection method is widely used for assessing experimental metastatic colonization of cancer cells, the overall metastatic burden in this *in vivo* assay is also influenced by tumor cell survival in the circulation as well as extravasation ability of tumor cells at the metastatic site. Furthermore, while *in vivo* studies involving human cancer cells necessitate the use of immunodeficient animals, since immune cells have a multitude of effects on OBs and OCLs in bone metastatic microenvironment thereby dictating the outgrowth behavior of cancer cells (43), fully immunocompetent mouse models are more physiologically relevant model systems. Therefore, in our next set of experiments,

we performed direct intratibial injection of control vs MRTF-knockdown D2A1 cells in syngeneic immunocompetent Balb/c mice. Consistent with our findings of MDA-231 study, 70% (7 out of 10) of mice subjected to intratibial injection of control D2A1 cells presented with metastatic growth in the bone (detectable by BLI signal) within 7 days after injection, compared to only 30% (3 out 10) mice injected with MRTF knockdown cells (**Fig 7D**). Consistent with these in vivo data, we additionally found that MRTF knockdown dramatically inhibits outgrowth of MDA-231 cells when seeded on devitalized bone surface prepared from mouse calvaria (**Figs 7E-F**). Collectively, these data underscore MRTF's importance in bone colonization of breast cancer cells.

DISCUSSION

In the present study, we report four major findings. First, while previous studies demonstrated MRTF-dependent changes in tumor-cell-intrinsic phenotypes (proliferation, migration and susceptibility to immune cell attack) (19-21), whether MRTF activity in tumor cells indirectly impacts other cells in the tumor microenvironment is not known. In this study, we uncover a novel tumor-cell-extrinsic function of MRTF in promoting osteoclastogenesis in a paracrine manner. Second, we establish CTGF as one of mediators of pro-osteoclastogenic paracrine action of MRTF in breast cancer cells. Although it is known that CTGF is one of the serum-induced early-responsive genes in cells (44), and its expression is induced in cultured cells when MRTF-A is overexpressed (32), CTGF is also regulated by other transcription factors (40). Therefore, to what extent basal CTGF expression is dependent on MRTF's action is not known. In this study, we show that MRTF is absolutely essential for maintaining the basal CTGF expression in cultured cells and further demonstrate a strong association between CTGF expression and MRTF gene signature in an actual human disease context. Third, we identify a host of additional cell-secreted immunoregulatory factors that are affected upon loss of MRTF expression in breast cancer cells providing additional mechanistic insights into how MRTF-deficiency in breast cancer cells could potentially interfere with osteoclastogenesis as depicted in **Fig 8**. Fourth, we demonstrate that MRTF is required for bone colonization of breast cancer cells. Collectively, these findings suggest that MRTF inhibition could be an effective strategy to diminish OCL formation and skeletal involvement in breast cancer.

OCL differentiation and activation is a multistep process that is dependent on a multitude of growth factors liberated from the bone matrix and secreted by tumor cells in the metastatic niche. This involves proliferation and differentiation of hematopoietic stem cells to RANK-/TRAP- OCL progenitor cells, differentiation of OCL progenitor cells to RANK+/TRAP+ mononuclear OCLs (a process that is dependent on the activities of NF-κb and NFATc transcription factors), and finally fusion of mononuclear OCLs to multi-nucleated and bone-resorption competent mature OCLs that are characterized by the expressions various markers including DC-Stamp, Atp6v0d2 (v-ATPase subunit d2), cathepsin K, and OSTM1 (osteoclastogenesis-associated transmembrane protein) (45). Our studies revealed that regardless of the MRTF expression status in breast cancer cells, exposure to tumor cell CM reduces the total cell count of BMDM cells (by ~50%) but enhances their intrinsic differentiation ability to multi-nucleated OCLs in an MRTF-dependent manner. Given that OCL differentiation efficiency of RANKL-stimulated BMDM culture is below 10%, we speculate that tumor cell-derived factors promote fusion of mono-nuclear OCLs, and this process is inhibited when MRTF expression is silenced in breast cancer cells. DC-Stamp, a transmembrane protein originally identified in dendritic cells, is essential for cell-cell fusion in OCLs (25, 46). Our studies showed that RANKL-induced DC-Stamp expression in BMDMs is prominently enhanced

(by ~3 fold) by secreted factors of breast cancer cells in an MRTF-dependent manner. CTGF plays a key role in both induction of and interaction with DC-Stamp resulting in multi-nuclear OCL formation (41). Since MRTF is critical for maintaining the basal expression of CTGF, MRTF's requirement for increased OCL differentiation efficiency of BMDMs elicited by tumor cell-derived factors may be partly due to enhanced fusion of mono-nuclear cells by a CTGF/DC-Stamp signaling axis. Since cell motility plays a key role in bringing mononuclear OCLs into close proximity aiding their fusion process (47), another possibility is that BMDM motility is impacted by exposure to tumor cell secreted factors in an MRTF-dependent manner. However, since OCL assessment in our studies was restricted to a fixed time-point (i.e. 4 days after RANKL stimulation) we cannot rule out MRTF's role in early aspects of OCL differentiation process. Additional time-course studies of RANK activation (and its downstream signaling readouts such as activation and sustenance of NF-Kb signaling) and expression of early-responsive genes (e.g. NFATc1 and ACP5) will provide additional insights.

Our studies clearly indicate that MRTF-depletion in breast cancer cells has a suppressive effect on OCL differentiation process through a paracrine action that extends beyond the effect of CTGF. To this end, RNA-seq analysis identified MRTF-dependent upregulation of pro-osteoclastogenic factors IL11 and FGF5 (these factors were not represented in Luminex assay). Our Luminex studies additionally discovered that MRTF-depletion in breast cancer cells leads to reduced secreted levels of several pro-osteoclastogenic cytokines (IL8, G-CSF, IL25, FLT3L, IL1α) with concomitant upregulation of anti-osteoclastogenic cytokines (IL1RA, IL27, GM-CSF and RANTES/CCL5). Between these factors, G-CSF downregulation upon MRTF knockdown was reproducible in both human and mouse breast cancer cells. Among the pro-osteoclastogenic factors identified by Luminex analyses, IL8 stimulates OCL differentiation through inducing RANK-induced NFATc1 activation in an autocrine-signaling manner (48). G-CSF accelerates osteoblast turnover and suppresses the expression OPG (a negative regulator of RANK/RANKL signaling) (49) while eliciting increased OCL activity and bone resorption in both cancer (50) and periodontitis models (51). Although FL3T3L can substitute for M-CSF in supporting OCL induction (52), since our studies were performed in cultures supplemented with M-CSF, we presume that reduced FL3TL secretion, if at all, has minimal role, in suppression of OCL differentiation in MRTF knockdown setting. Among the anti-osteoclastogenic factors, IL27 is known to inhibit RANKL-induced signaling pathway (53). IL1RA (IL1 receptor antagonist) inhibits the signaling elicited by IL1, an inducer of RANKL expression as well as an activator of various hallmark gene expression programs [NFκβ, p38, ERK] required for OCL differentiation (54)). Therefore, we will need to investigate potential contributions of these select candidate differentially abundant cytokines and changes in associated signaling pathways as additional future directions of mechanistic investigations underlying MRTF-regulated paracrine control of OCL differentiation. Although beyond the scope of the present study, given the concordance of downregulation of G-CSF and possibly IL1 signaling (marked by either downregulation of IL1α or upregulation of IL1RA) between human and mouse breast cancer cell lines, it will be important to design combinatorial rescue studies to determine whether exogenous supplementation of IL1 and/or G-CSF with CTGF fully recoups the OCL differentiation defect induced by MRTF-depletion in breast cancer cells.

We previously showed that *in vivo* administration of CCG-1423, a small molecule that is widely used to inhibit MRTF's function (55-57), dramatically reduces development of skeletal metastases following systemic inoculation of breast cancer cells (20). However, CCG-1423 or its derivative compounds have poly-pharmacology and are known to target other proteins (example: MICAL and pirin) (58, 59). In fact,

CCG compounds bind to pirin at a much higher affinity than to MRTF. This is further underscored by our own unpublished RNA-seq findings of extremely broad transcriptional changes induced by CCG-1423 in breast cancer cells with only ~ 4% of those genes transcriptionally altered by CCG-1423 being MRTF-related (data not shown). Furthermore, in an *in vivo* administration setting, CCG compound's action is targeted globally in a non-cell type-specific manner. Therefore, to what extent MRTF-activity in tumor cells contributes to bone colonization remained unclear in that study, which is now resolved by genetic proof-of-concept for MRTF's role in bone colonization of breast cancer cells as demonstrated in this study. Since our experimental metastasis assessments were restricted to a relatively early time-point after tumor cell inoculation in this study, it is likely that reduced frequency of bone colonization of MRTF-knockdown cells is primarily due to their defect in proliferation (as suggested by our proliferation assay results) and/or survival. However, our main finding that loss-of-function of MRTF in tumor cells negatively impacts RANKL-induced OCL differentiation is still significant because of its implication in osteolysis-induced feed-forward loop to drive tumor cell growth in the bone microenvironment particularly in the advanced stage of metastatic growth of cancer cells.

Finally, we acknowledge that there are limitations of the present study. For example, this study models only the unidirectional signaling from cancer cells to OCLs and does not represent the complex multicellular crosstalk between osteoblasts, cancer cells and OCLs of the actual tumor microenvironment. Second, we did not investigate whether MRTF has any role in influencing the intrinsic OCL differentiation ability of BMDMs. Addressing these lines of questions using advanced model systems incorporating multiple cell types and further in vivo validation should be the focus for future investigations.

EXPERIMENTAL PROCEDURES

Animal Studies. All animal experiments were conducted in compliance with an approved IACUC protocol, according to University of Pittsburgh Division of Laboratory Animal Resources guidelines. Briefly, 10^5 MDA-231 cells, suspended in 100 µL PBS, were injected into the left cardiac ventricle of fully anesthetized 5-week-old female NSG mice. For intratibial injections, 2.5×10^4 D2.A1 cells, suspended in 20 µL PBS, were injected into the right tibia of fully anesthetized 5-week-old female immunocompetent Balb/c mice. Bioluminescence imaging (BLI) of anesthetized mice was performed with IVIS Spectrum 15 minutes after intraperitoneal injection of D-luciferin.

Cell culture and OCL differentiation assay. Generation and culture of variants of MDA-231, stably co-expressing GFP and luciferase, and various MRTF-A constructs have been previously described (20). D2.A1 cells stably expressing luciferase (a gift from Dr. William Schiemann, Case Western Reserve University) were cultured in DMEM media (Lonza, catalog# BW12-604F) supplemented with 10% (v/v) FBS and 1% antibiotics (100 U/ml penicillin and 100 µg/mL streptomycin). For stable silencing of MRTF isoforms, MDA-231 and D2A1 cells were transduced with lentivirus encoding either MRTF-A/B shRNA (Vectorbuilder vector ID - VB200825-1246dwj) or non-targeting control shRNA (Vectorbuilder vector ID - VB151023-10034) and selected with puromycin. Primary BMDMs were isolated from the long bones of female FVB mice and cultured in αMEM medium supplemented with 10% (v/v) fetal bovine serum (FBS; Corning, catalog# MT35011CV) and 1% antibiotics (100 U/ml penicillin and 100 µg/ml streptomycin; Thermo Fisher, catalog# 15070063) as described previously (60). Primary BMDMs were seeded in the wells of a 96 wells plate in triplicate and expanded in αMEM supplemented with M-CSF (20 ng/mL) for 3 days to generate OCL progenitor (OCLp) cells. OCL differentiation was induced by additional 4 days of

culture in the presence of RANKL (10 ng/mL) and M-CSF (10 ng/mL), with or without the addition of breast cancer cell CM at a 10% v/v ratio. To prepare CM, breast cancer cells were seeded in a 10 cm plate and cultured in serum containing media for 4 days prior to collection. For CTGF rescue studies, CTGF (PeproTech, 120-19) was added to the BMDM culture at either 50 ng/ml or 100 ng/ml concentration at the time of RANKL stimulation and continued until the end of experiments. To assess OCL differentiation, cells were fixed with 37% formaldehyde for 15 minutes, washed with PBS and stained using leukocyte acid phosphatase kit (Sigma-Aldrich, 387A-1KT) following the manufacturer's instructions. OCLs (marked by TRAP+ multinucleated cells with three or more nuclei) were counted using the "OC_Finder" program which uses an automated cell segmentation approach before applying deep learning to classify the cells as either OCLs or non-OCLs (61). Total number of cells was counted using ImageJ.

2D Proliferation Assay and protein quantification. Twenty-five thousand MDA-231 or D2A1 cells were seeded in the wells of a 6-well plate and cultured in Phenol free DMEM media (ThermoFisher, catalog# 31053028) supplemented with 10% (v/v) FBS and 1% antibiotics (100 U/ml penicillin and 100 µg/mL streptomycin). Cells were imaged and counted using Millicell DCI Digital Cell Imager four consecutive days starting from the day after cell seeding. Media samples were also taken daily and quantified for protein content using biocinchoninic acid assay.

Calvaria preparation/tumor cell outgrowth assay. Female C57Bl/6 post-natal day 21 mice were injected intraperitoneally with 20 mg/kg Alizarin complexone dihydrate (CAS 455303-00-1, 2.0 mg/ml in bicarbonate buffer) and sacrificed 24 hours post injection. Calvaria were immediately excised and placed in phosphate buffered saline. The periosteum was removed by scraping with a scalpel. Calvaria were then digested in 0.5 mg/mL collagenase (Sigma Aldrich, catalog #C9697-50), 0.25% trypsin-EDTA for 10 minutes at a time at 37ºC and stored in PBS at -20°C until used. Two thousand cells were seeded in duplicates in a 96-well plate on approximately 2 mm x 2 mm sized squares of calvaria. After 72 hours of culture, cells were imaged at 4x magnification and outgrowth was quantified by the total calvarial area covered by GFP+ cells using ImageJ.

RNA extraction, quantitative RT-PCR and RNA-sequencing. Total RNA was extracted from either 2D or matrigel-on-top (MoT) 3D (protocol for MoT 3D culture is detailed in (20)) cultures using RNeasy mini kit (Qiagen, catalog #74104) according to the manufacturer's instructions. Complementary DNA (cDNA) was synthesized from 1 ug of RNA using the QuantiTect reverse transcription kit (Qiagen, catalog #205311) following the manufacturer's instructions. Each PCR was prepared with 50 ng of cDNA, 12.5 µL of SYBR Select Master Mix (ThermoFisher, catalog #4472903), 1 µM forward and reverse primers, and water for a total volume of 25 µL. Thermal cycling and data analysis were performed using the StepOne Plus Real-Time PCR System and StepOne Software (Applied Biosystems) to detect quantitative mRNA expression of Cathepsin-K and DC-STAMP (primer sequences are listed in **supplementary Table S3**). RNA sequencing was performed at the University of Pittsburgh HSCRF Genomics Research Core. Fastq files from SRP097696 archive were downloaded using SRA Toolkit version 2.9.2. Transcripts from the Ensembl v.93 transcriptome (hg38) were quantified with Salmon v0.14.0. Gene-level expression was calculated using tximport v.1.12.0 and differential gene expression was calculated with DESeq2 v.1.24.0. Quality control principal component and heatmap plots demonstrated one potential outlier sample, which was removed prior to final differential gene expression analysis (these data are deposited in GEO (GSE253047)).

Protein extraction and Western blotting. Cell lysates were prepared by a modified RIPA buffer (25 mM Tris–HCL: pH 7.5, 150 mM NaCl, 1% (v/v) NP-40, 5% (v/v) glycerol), 1 mM EDTA, 50 mM NaF, 1 mM sodium pervanadate, and protease inhibitors (Sigma, catalog P8340) supplemented with 6× sample buffer diluted to 1× with the final SDS concentration in the lysis buffer equivalent to 2%. Conditions for the various antibodies were: polyclonal MRTF-A (Cell Signaling, catalog #14760S; 1:1000), MRTF-B (Cell Signaling, catalog #14613S; 1:1000), polyclonal GAPDH (Sigma, catalog #G9545, 1:2000), polyclonal CTGF (Abcam, catalog #ab6992), monoclonal Tubulin (Sigma, T9026, 1:1000). monoclonal anti-rabbit HRP (Jackson Immunoresearch, catalog #211–032-171, 1:1000), and polyclonal anti-mouse HRP (BD Biosciences, catalog #554002, 1:1000).

Cytokine Analyses. CM harvested from 10 cm culture plates and concentrated to 100 µL was probed for cytokine/chemokine expression levels by HD48A (48-plex human discovery assay) and MD32 (32-plex mouse discovery assay) Luminex panels using a service provided by Eve Technologies (Calgary, AB, Canada). Values were normalized to the average value of the control group per analyte basis.

Statistics. All statistical tests were performed using GraphPad Prism 9 software. ANOVA (for more than 2 groups) and Student's t-test (for 2 groups) were performed for comparing the means between various experimental groups. For ANOVA, we performed Tukey's post hoc test for individual group comparisons. A p-value less than 0.05 was considered statistically significant.

DATA AVAILABILITY

RNA-sequencing data has been submitted to GEO (GSE253047)**.** All other data are included in the manuscript and supporting information.

SUPPORTING INFORMATION

The article contains supporting information.

ACKNOWLDEGMENTS

DG was supported by a National Cancer Center fellowship, NCI K99-CA267180 and T32-HL129964. Work in the Roy lab was supported by grants from the NIH (R01CA248873, R01CA271095, and R21EY032632). Fangyuan Chen was a former visiting research scholar at the University of Pittsburgh School of Medicine supported by funds from The China Scholarship Council and Tsinghua University.

AUTHOR CONTRIBUTION

PC and DG performed experiments, analyzed data, and wrote manuscript; DB, NW and FC performed data analyses, JT contributed to generation of experimental tools; AVL oversaw some aspects of data analyses, DLG conceived study design and supervised some aspects of the project, PR conceived the overall study design, supervised the project, oversaw experiments, edited/wrote manuscript and acquired funding.

CONFLICT OF INTEREST: The authors declare no conflict of interest.

Figure legends

Figure 1. Dual knockdown of MRTF expression in breast cancer cell lines. A-B) Representative immunoblots of total cell lysates of MDA-231 and D2.A1 cells (*panel A;* tubulin blot: loading control) and quantifications of immunoblot data (*panel B*) demonstrating shRNA-mediated stable knockdown of MRTF isoforms in both cell lines. **C)** Proliferation curves of control vs stable MRTF-A/B knockdown MDA-231 and D2A1 cells in 2D tissue culture (relative to the value measured for control groups of cells on day 1); arrow indicates the day conditioned media (CM) was harvested for subsequent OCL differentiation experiments. All data are summarized from 3 independent experiments; *: $p<0.05$; **: $p<0.01$).

Figure 2. Tumor cell-derived factors promote RANKL-induced OCL differentiation of BMDMs in an MRTF-dependent manner A) Schematic of the experimental protocol of RANKL-induced OCL differentiation with or without tumor cell CM supplementation. **B)** Representative images of TRAP-stained BMDM cultures in the absence or presence of RANKL (with or without MDA-231 CM supplementation; C- control shRNA; M- MRTF-A/B shRNA; scale bar in the inset images – 200 µm). **C-D)** Quantifications of total cell count (*panel C*) and OCL differentiation indices (*panel D*) of BMDM cultures for the indicated treatment groups (data summarized from 4 and 3 independent experiments for CM treatment from MDA-231 and D2.A1, cells respectively (* $p<0.05$, **: $p<0.01$, and **** $p<0.0001$). **E**) Quantitative RT-qPCR analyses show the fold-changes in the mRNA expression levels of DC-Stamp and Cathepsin-K in BMDM cultures subjected to the indicated treatments (fold changes normalized to the expression values for RANKL-alone treatment group; data summarized from 3 independent experiments; * $p<0.05$, and **: $p<0.01$).

Figure 3: **Both SAP-domain and SRF-related functions of MRTF are important for tumor-cell-directed paracrine modulation of OCL differentiation.** Quantifications of OCL differentiation indices (*panel A*) and total cell count (*panel B*) of RANKL-stimulated BMDMs without or with supplementation of CM derived from the 2D cultures of control vs various stable MRTF-A (either WT or specific functional mutants) overexpressing sublines of MDA-231 cells (data summarized from 3 independent experiments, **** $p<0.0001$; N.S – not significant).

Figure 4. Identification of candidate bone metastasis-associated genes inducible by MRTF. A) TPM (transcripts per million – normalized to housekeeping genes) of candidate bone metastasis associated genes (IL11, CTGF, FGF5) based on RNA-sequencing data of 2D and 3D cultures of MDA-231 cells subjected to acute doxycycline-induced overexpression of wild-type (WT) vs various mutant forms of MRTF-A. **B)** Correlation between select genes and MRTF gene signature score (GSS) in TCGA, MRTABRIC and SCANB databases (Spearman's co-efficient (S) and p-values are included for each of these analyses). **C)** Correlation between CTGF and MRTF-A mRNA expression in human breast cancer samples (based on TCGA data analyses).

Figure 5. **CTGF is a mediator of MRTF-dependent paracrine regulation of OCL differentiation by breast cancer cells. A-B)** CTGF immunoblots and the associated quantification of the immunoblot data of total cell lysates of MDA-231 (*panel A*) and D2A1 (*panel B*) cells with or without stable knockdown of MRTF isoforms (GAPDH and tubulin blots serve as loading controls). **C)** Representative CTGF immunoblot and the associated quantification control vs various MRTF-A (WT and functional mutants)

overexpressing sublines MDA-231 cells. **D-E)** Quantification of OCL differentiation index (*panel D)* and total cell count (*panel E*) of RANKL-stimulated BMDM cultures without or with supplementation of MDA-231 CM and/or recombinant CTGF at the indicated concentrations. All data presented here are summarized from 3 independent experiments; *: $p<0.05$, **: $p<0.01$, *** $p<0.001$, and **** $p<0.0001$).

Figure 6. MRTF-dependent changes in secreted immunomodulatory factors. Heat plots of differentially abundant cytokines/chemokines in the CM of control vs stable MRTF knockdown (KD) MDA-231 (*panel A*) and D2A1 (*panel B*) cultures. Fold changes and p-values for differentially abundant cytokines/chemokines with pro- vs anti-osteoclastogenic activities are indicated below.

Figure 7. MRTF depletion impairs experimental bone colonization of breast cancer cells *in vivo*. A-C) Representative endpoint BLI images (*panel A*) NSG mice 2 weeks after intracardiac injection of control vs MRTF-A/B knockdown MDA-231 cells (asterisks indicate skeletal metastasis). Panel B summarizes the distant metastasis quantification based on the BLI signaling readouts (data normalized to the control group). Hematoxylin and Eosin staining of BLI signal-positive bones in panel C confirms presence of metastases (indicated by the arrow) harvested from mice injected with control shRNA-bearing cells. Scale bar represents 200 μm. **D)** BLI images of immunocompetent Balb/c mice 1 week after intratibial injection of control vs MRTF-A/B knockdown D2.A1 cells. **E)** Representative fluorescence images of GFP+ control and MRTF-A/B shRNA expressing MDA-231 cells 72 hrs after seeding on alizarin red+ mouse calvarial bone. **F)** Quantification of area of bone covered with GFP+ cells 72 hours post-seeding (data summarized from 3 independent experiments, **** $p<0.0001$; scale bar – 50 μm). Non-flat nature and autofluorescence of calvarial bone punches account for the sub-optimal quality of fluorescence images.

Figure 8. **Proposed schematic model.** MRTF activity in breast cancer cells promotes OCL differentiation through a paracrine action that involves the action of CTGF and other OCL-regulatory factors.

REFERENCES

1. Shibue, T., andWeinberg, R. A. (2011) Metastatic colonization: settlement, adaptation and propagation of tumor cells in a foreign tissue environment Seminars in cancer biology **21**, 99-106 10.1016/j.semcancer.2010.12.003
2. Engers, R., andGabbert, H. E. (2000) Mechanisms of tumor metastasis: cell biological aspects and clinical implications Journal of cancer research and clinical oncology **126**, 682-692 10.1007/s004320000148
3. Qiao, R. Q., Zhang, H. R., Ma, R. X., Li, R. F., andHu, Y. C. (2022) Prognostic Factors for Bone Survival and Functional Outcomes in Patients With Breast Cancer Spine Metastases Technol Cancer Res Treat **21**, 15330338221122642 10.1177/15330338221122642
4. Kennecke, H., Yerushalmi, R., Woods, R., Cheang, M. C., Voduc, D., Speers, C. H. *et al.* (2010) Metastatic behavior of breast cancer subtypes Journal of clinical oncology : official journal of the American Society of Clinical Oncology **28**, 3271-3277 10.1200/jco.2009.25.9820
5. Chen, Y. C., Sosnoski, D. M., andMastro, A. M. (2010) Breast cancer metastasis to the bone: mechanisms of bone loss Breast cancer research : BCR **12**, 215 10.1186/bcr2781
6. Weidle, U. H., Birzele, F., Kollmorgen, G., andRüger, R. (2016) Molecular Mechanisms of Bone Metastasis Cancer Genomics Proteomics **13**, 1-12,
7. Boyce, B. F., andXing, L. (2008) Functions of RANKL/RANK/OPG in bone modeling and remodeling Arch Biochem Biophys **473**, 139-146 10.1016/j.abb.2008.03.018
8. Tsuda, E., Goto, M., Mochizuki, S., Yano, K., Kobayashi, F., Morinaga, T., andHigashio, K. (1997) Isolation of a novel cytokine from human fibroblasts that specifically inhibits osteoclastogenesis Biochemical and biophysical research communications **234**, 137-142 10.1006/bbrc.1997.6603
9. Yasuda, H., Shima, N., Nakagawa, N., Yamaguchi, K., Kinosaki, M., Mochizuki, S. *et al.* (1998) Osteoclast differentiation factor is a ligand for osteoprotegerin/osteoclastogenesis-inhibitory factor and is identical to TRANCE/RANKL Proceedings of the National Academy of Sciences of the United States of America **95**, 3597-3602 10.1073/pnas.95.7.3597
10. Nguyen, D. X., Bos, P. D., andMassagué, J. (2009) Metastasis: from dissemination to organ-specific colonization Nature reviews **9**, 274-284 10.1038/nrc2622
11. David Roodman, G., andSilbermann, R. (2015) Mechanisms of osteolytic and osteoblastic skeletal lesions Bonekey Rep **4**, 753 10.1038/bonekey.2015.122
12. Kang, Y., Siegel, P. M., Shu, W., Drobnjak, M., Kakonen, S. M., Cordón-Cardo, C. *et al.* (2003) A multigenic program mediating breast cancer metastasis to bone Cancer cell **3**, 537-549 10.1016/s1535-6108(03)00132-6
13. Casimiro, S., Ferreira, A. R., Mansinho, A., Alho, I., andCosta, L. (2016) Molecular Mechanisms of Bone Metastasis: Which Targets Came from the Bench to the Bedside? Int J Mol Sci **17**, 10.3390/ijms17091415
14. Olson, E. N., andNordheim, A. (2010) Linking actin dynamics and gene transcription to drive cellular motile functions Nature reviews Molecular cell biology **11**, 353-365 10.1038/nrm2890
15. Gasparics, Á., andSebe, A. (2018) MRTFs- master regulators of EMT Developmental dynamics : an official publication of the American Association of Anatomists **247**, 396-404 10.1002/dvdy.24544
16. Gau, D., andRoy, P. (2018) SRF'ing and SAP'ing - the role of MRTF proteins in cell migration Journal of cell science **131**, 10.1242/jcs.218222
17. Sun, Y., Boyd, K., Xu, W., Ma, J., Jackson, C. W., Fu, A. *et al.* (2006) Acute myeloid leukemia-associated Mkl1 (Mrtf-a) is a key regulator of mammary gland function Molecular and cellular biology **26**, 5809-5826 10.1128/mcb.00024-06

18. Oh, J., Richardson, J. A., andOlson, E. N. (2005) Requirement of myocardin-related transcription factor-B for remodeling of branchial arch arteries and smooth muscle differentiation Proceedings of the National Academy of Sciences of the United States of America **102**, 15122-15127 10.1073/pnas.0507346102
19. Medjkane, S., Perez-Sanchez, C., Gaggioli, C., Sahai, E., andTreisman, R. (2009) Myocardin-related transcription factors and SRF are required for cytoskeletal dynamics and experimental metastasis Nature cell biology **11**, 257-268 10.1038/ncb1833
20. Gau, D., Chawla, P., Eder, I., andRoy, P. (2022) Myocardin-related transcription factor's interaction with serum-response factor is critical for outgrowth initiation, progression, and metastatic colonization of breast cancer cells FASEB Bioadv **4**, 509-523 10.1096/fba.2021-00113
21. Tello-Lafoz, M., Srpan, K., Sanchez, E. E., Hu, J., Remsik, J., Romin, Y. *et al.* (2021) Cytotoxic lymphocytes target characteristic biophysical vulnerabilities in cancer Immunity **54**, 1037-1054.e1037 10.1016/j.immuni.2021.02.020
22. Kirstein, B., Chambers, T. J., andFuller, K. (2006) Secretion of tartrate-resistant acid phosphatase by osteoclasts correlates with resorptive behavior Journal of cellular biochemistry **98**, 1085-1094 10.1002/jcb.20835
23. Ethiraj, L. P., Fong, E. L. S., Liu, R., Chan, M., Winkler, C., andCarney, T. J. (2022) Colorimetric and fluorescent TRAP assays for visualising and quantifying fish osteoclast activity Eur J Histochem **66**, 10.4081/ejh.2022.3369
24. Saftig, P., Hunziker, E., Everts, V., Jones, S., Boyde, A., Wehmeyer, O. *et al.* (2000) Functions of cathepsin K in bone resorption. Lessons from cathepsin K deficient mice Advances in experimental medicine and biology **477**, 293-303 10.1007/0-306-46826-3_32
25. Yagi, M., Miyamoto, T., Sawatani, Y., Iwamoto, K., Hosogane, N., Fujita, N. *et al.* (2005) DC-STAMP is essential for cell-cell fusion in osteoclasts and foreign body giant cells The Journal of experimental medicine **202**, 345-351 10.1084/jem.20050645
26. Ljusberg, J., Wang, Y., Lång, P., Norgård, M., Dodds, R., Hultenby, K. *et al.* (2005) Proteolytic excision of a repressive loop domain in tartrate-resistant acid phosphatase by cathepsin K in osteoclasts J Biol Chem **280**, 28370-28381 10.1074/jbc.M502469200
27. Cen, B., Selvaraj, A., Burgess, R. C., Hitzler, J. K., Ma, Z., Morris, S. W., andPrywes, R. (2003) Megakaryoblastic leukemia 1, a potent transcriptional coactivator for serum response factor (SRF), is required for serum induction of SRF target genes Molecular and cellular biology **23**, 6597-6608, http://www.ncbi.nlm.nih.gov/pubmed/12944485
28. Gurbuz, I., Ferralli, J., Roloff, T., Chiquet-Ehrismann, R., andAsparuhova, M. B. (2014) SAP domain-dependent Mkl1 signaling stimulates proliferation and cell migration by induction of a distinct gene set indicative of poor prognosis in breast cancer patients Molecular cancer **13**, 22 10.1186/1476-4598-13-22
29. Asparuhova, M. B., Ferralli, J., Chiquet, M., andChiquet-Ehrismann, R. (2011) The transcriptional regulator megakaryoblastic leukemia-1 mediates serum response factor-independent activation of tenascin-C transcription by mechanical stress Faseb j **25**, 3477-3488 10.1096/fj.11-187310
30. Asparuhova, M. B., Secondini, C., Ruegg, C., andChiquet-Ehrismann, R. (2015) Mechanism of irradiation-induced mammary cancer metastasis: A role for SAP-dependent Mkl1 signaling Molecular oncology **9**, 1510-1527 10.1016/j.molonc.2015.04.003
31. Savci-Heijink, C. D., Halfwerk, H., Hooijer, G. K., Horlings, H. M., Wesseling, J., andvan de Vijver, M. J. (2015) Retrospective analysis of metastatic behaviour of breast cancer subtypes Breast cancer research and treatment **150**, 547-557 10.1007/s10549-015-3352-0
32. Hinkel, R., Trenkwalder, T., Petersen, B., Husada, W., Gesenhues, F., Lee, S. *et al.* (2014) MRTF-A controls vessel growth and maturation by increasing the expression of CCN1 and CCN2 Nature communications **5**, 3970 10.1038/ncomms4970

33. Choi, Y., Yoo, J. H., Lee, J. H., Lee, Y., Bae, M. K., Kim, Y. D., andKim, H. J. (2020) Connective tissue growth factor (CTGF) regulates the fusion of osteoclast precursors by inhibiting Bcl6 in periodontitis Int J Med Sci **17**, 647-656 10.7150/ijms.41075
34. McCoy, E. M., Hong, H., Pruitt, H. C., andFeng, X. (2013) IL-11 produced by breast cancer cells augments osteoclastogenesis by sustaining the pool of osteoclast progenitor cells BMC cancer **13**, 16 10.1186/1471-2407-13-16
35. Aukes, K., Forsman, C., Brady, N. J., Astleford, K., Blixt, N., Sachdev, D. *et al.* (2017) Breast cancer cell-derived fibroblast growth factors enhance osteoclast activity and contribute to the formation of metastatic lesions PloS one **12**, e0185736 10.1371/journal.pone.0185736
36. Pereira, B., Chin, S.-F., Rueda, O. M., Vollan, H.-K. M., Provenzano, E., Bardwell, H. A. *et al.* (2016) The somatic mutation profiles of 2,433 breast cancers refine their genomic and transcriptomic landscapes Nature communications **7**, 11479 10.1038/ncomms11479
37. Ciriello, G., Gatza, M. L., Beck, A. H., Wilkerson, M. D., Rhie, S. K., Pastore, A. *et al.* (2015) Comprehensive Molecular Portraits of Invasive Lobular Breast Cancer Cell **163**, 506-519 10.1016/j.cell.2015.09.033
38. Brueffer, C., Gladchuk, S., Winter, C., Vallon-Christersson, J., Hegardt, C., Häkkinen, J. *et al.* (2020) The mutational landscape of the SCAN-B real-world primary breast cancer transcriptome EMBO molecular medicine **12**, e12118 10.15252/emmm.202012118
39. Hänzelmann, S., Castelo, R., andGuinney, J. (2013) GSVA: gene set variation analysis for microarray and RNA-seq data BMC bioinformatics **14**, 7 10.1186/1471-2105-14-7
40. Cheng, J. C., Wang, E. Y., Yi, Y., Thakur, A., Tsai, S. H., andHoodless, P. A. (2018) S1P Stimulates Proliferation by Upregulating CTGF Expression through S1PR2-Mediated YAP Activation Mol Cancer Res **16**, 1543-1555 10.1158/1541-7786.Mcr-17-0681
41. Nishida, T., Emura, K., Kubota, S., Lyons, K. M., andTakigawa, M. (2011) CCN family 2/connective tissue growth factor (CCN2/CTGF) promotes osteoclastogenesis via induction of and interaction with dendritic cell-specific transmembrane protein (DC-STAMP) J Bone Miner Res **26**, 351-363 10.1002/jbmr.222
42. Amarasekara, D. S., Yun, H., Kim, S., Lee, N., Kim, H., andRho, J. (2018) Regulation of Osteoclast Differentiation by Cytokine Networks Immune Netw **18**, https://doi.org/10.4110/in.2018.18.e8
43. Chen, S., Lei, J., Mou, H., Zhang, W., Jin, L., Lu, S. *et al.* (2024) Multiple influence of immune cells in the bone metastatic cancer microenvironment on tumors Front Immunol **15**, 1335366 10.3389/fimmu.2024.1335366
44. Herdegen, T., andLeah, J. D. (1998) Inducible and constitutive transcription factors in the mammalian nervous system: control of gene expression by Jun, Fos and Krox, and CREB/ATF proteins Brain Res Brain Res Rev **28**, 370-490 10.1016/s0165-0173(98)00018-6
45. Amarasekara, D. S., Yun, H., Kim, S., Lee, N., Kim, H., andRho, J. (2018) Regulation of Osteoclast Differentiation by Cytokine Networks Immune Netw **18**, e8 10.4110/in.2018.18.e8
46. Yagi, M., Miyamoto, T., Toyama, Y., andSuda, T. (2006) Role of DC-STAMP in cellular fusion of osteoclasts and macrophage giant cells J Bone Miner Metab **24**, 355-358 10.1007/s00774-006-0697-9
47. Søe, K. (2020) Osteoclast Fusion: Physiological Regulation of Multinucleation through Heterogeneity-Potential Implications for Drug Sensitivity Int J Mol Sci **21**, 10.3390/ijms21207717
48. Kopesky, P., Tiedemann, K., Alkekhia, D., Zechner, C., Millard, B., Schoeberl, B., andKomarova, S. V. (2014) Autocrine signaling is a key regulatory element during osteoclastogenesis Biol Open **3**, 767-776 10.1242/bio.20148128
49. Christopher, M. J., andLink, D. C. (2008) Granulocyte colony-stimulating factor induces osteoblast apoptosis and inhibits osteoblast differentiation J Bone Miner Res **23**, 1765-1774 10.1359/jbmr.080612

50. Hirbe, A. C., Uluçkan, O., Morgan, E. A., Eagleton, M. C., Prior, J. L., Piwnica-Worms, D. *et al.* (2007) Granulocyte colony-stimulating factor enhances bone tumor growth in mice in an osteoclast-dependent manner Blood **109**, 3424-3431 10.1182/blood-2006-09-048686
51. Yu, H., Zhang, T., Lu, H., Ma, Q., Zhao, D., Sun, J., andWang, Z. (2021) Granulocyte colony-stimulating factor (G-CSF) mediates bone resorption in periodontitis BMC Oral Health **21**, 299 10.1186/s12903-021-01658-1
52. Lean, J. M., Fuller, K., andChambers, T. J. (2001) FLT3 ligand can substitute for macrophage colony-stimulating factor in support of osteoclast differentiation and function Blood **98**, 2707-2713 10.1182/blood.v98.9.2707
53. Furukawa, M., Takaishi, H., Takito, J., Yoda, M., Sakai, S., Hikata, T. *et al.* (2009) IL-27 abrogates receptor activator of NF-kappa B ligand-mediated osteoclastogenesis of human granulocyte-macrophage colony-forming unit cells through STAT1-dependent inhibition of c-Fos J Immunol **183**, 2397-2406 10.4049/jimmunol.0802091
54. Kim, J. H., Jin, H. M., Kim, K., Song, I., Youn, B. U., Matsuo, K., andKim, N. (2009) The mechanism of osteoclast differentiation induced by IL-1 J Immunol **183**, 1862-1870 10.4049/jimmunol.0803007
55. Hayashi, K., Watanabe, B., Nakagawa, Y., Minami, S., andMorita, T. (2014) RPEL proteins are the molecular targets for CCG-1423, an inhibitor of Rho signaling PloS one **9**, e89016 10.1371/journal.pone.0089016
56. Kobayashi, M., Tokuda, K., Kobayashi, Y., Yamashiro, C., Uchi, S. H., Hatano, M., andKimura, K. (2019) Suppression of Epithelial-Mesenchymal Transition in Retinal Pigment Epithelial Cells by an MRTF-A Inhibitor Investigative ophthalmology & visual science **60**, 528-537 10.1167/iovs.18-25678
57. Song, M., Zhang, Y., Sun, Y., Kong, M., Han, S., Wang, C. *et al.* (2022) Inhibition of RhoA/MRTF-A signaling alleviates nucleus pulposus fibrosis induced by mechanical stress overload Connect Tissue Res **63**, 53-68 10.1080/03008207.2021.1952193
58. Lisabeth, E. M., Kahl, D., Gopallawa, I., Haynes, S. E., Misek, S. A., Campbell, P. L. *et al.* (2019) Identification of Pirin as a Molecular Target of the CCG-1423/CCG-203971 Series of Antifibrotic and Antimetastatic Compounds ACS Pharmacol Transl Sci **2**, 92-100 10.1021/acsptsci.8b00048
59. Lundquist, M. R., Storaska, A. J., Liu, T. C., Larsen, S. D., Evans, T., Neubig, R. R., andJaffrey, S. R. (2014) Redox modification of nuclear actin by MICAL-2 regulates SRF signaling Cell **156**, 563-576 10.1016/j.cell.2013.12.035
60. Allen-Gondringer, A., Gau, D., Varghese, C., Boone, D., Stolz, D., Larregina, A., andRoy, P. (2023) Vascular endothelial cell-specific disruption of the profilin1 gene leads to severe multiorgan pathology and inflammation causing mortality PNAS Nexus **2**, pgad305 10.1093/pnasnexus/pgad305
61. Wang, X., Kittaka, M., He, Y., Zhang, Y., Ueki, Y., andKihara, D. (2022) OC_Finder: Osteoclast segmentation, counting, and classification using watershed and deep learning Front Bioinform **2**, 10.3389/fbinf.2022.819570

Chawla et al. Figure 1

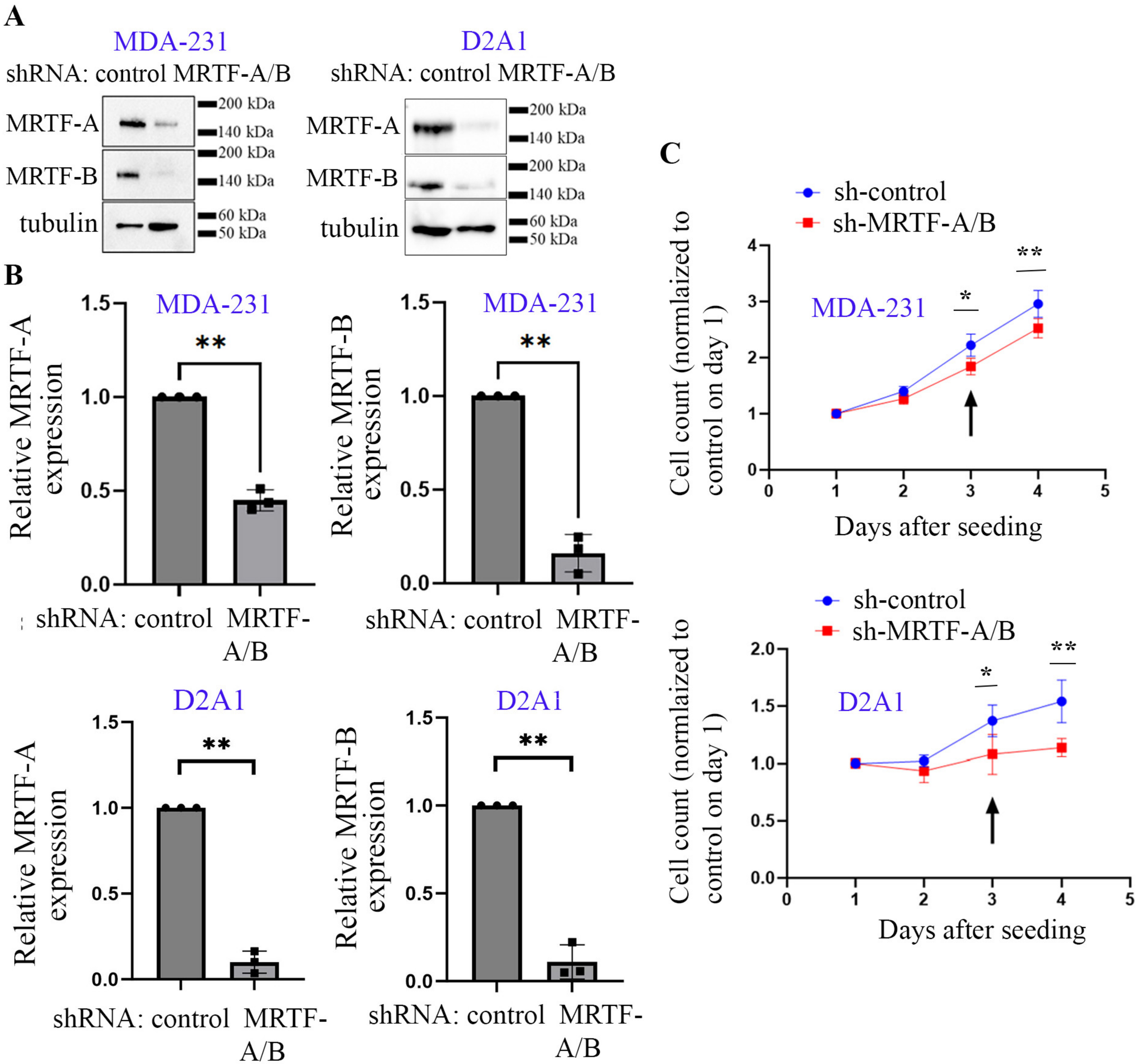

Chawla et al. Figure 2

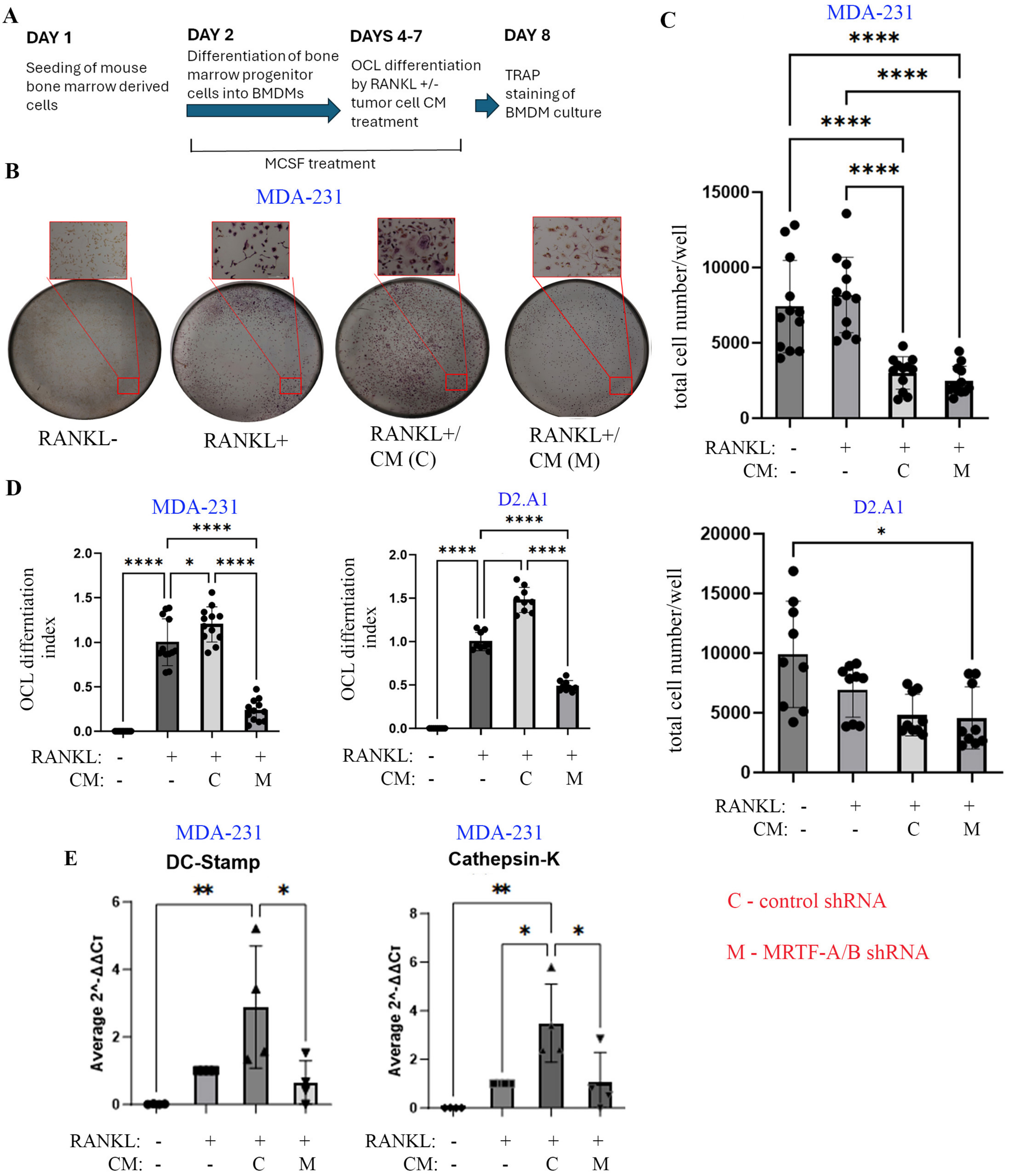

Chawla et al. Figure 3

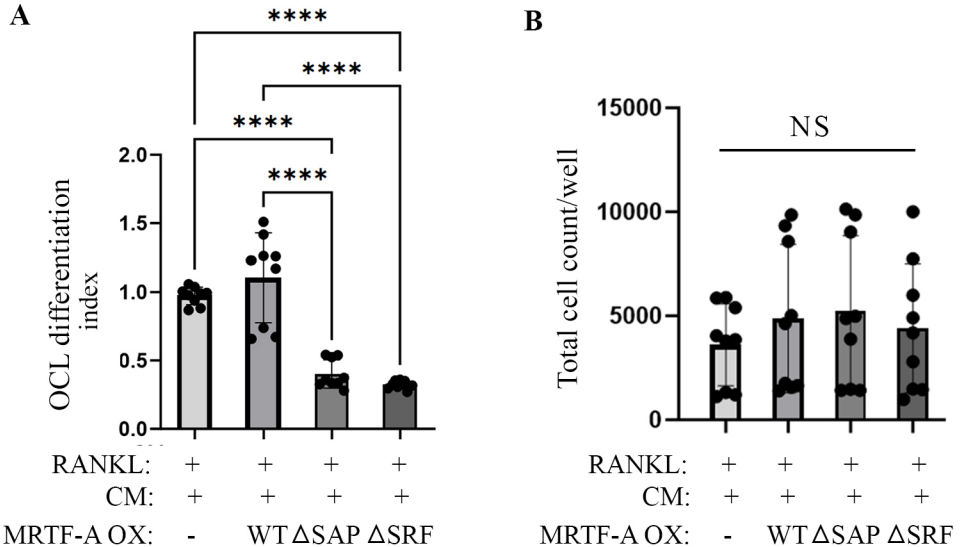

Chawla et al. Figure 4

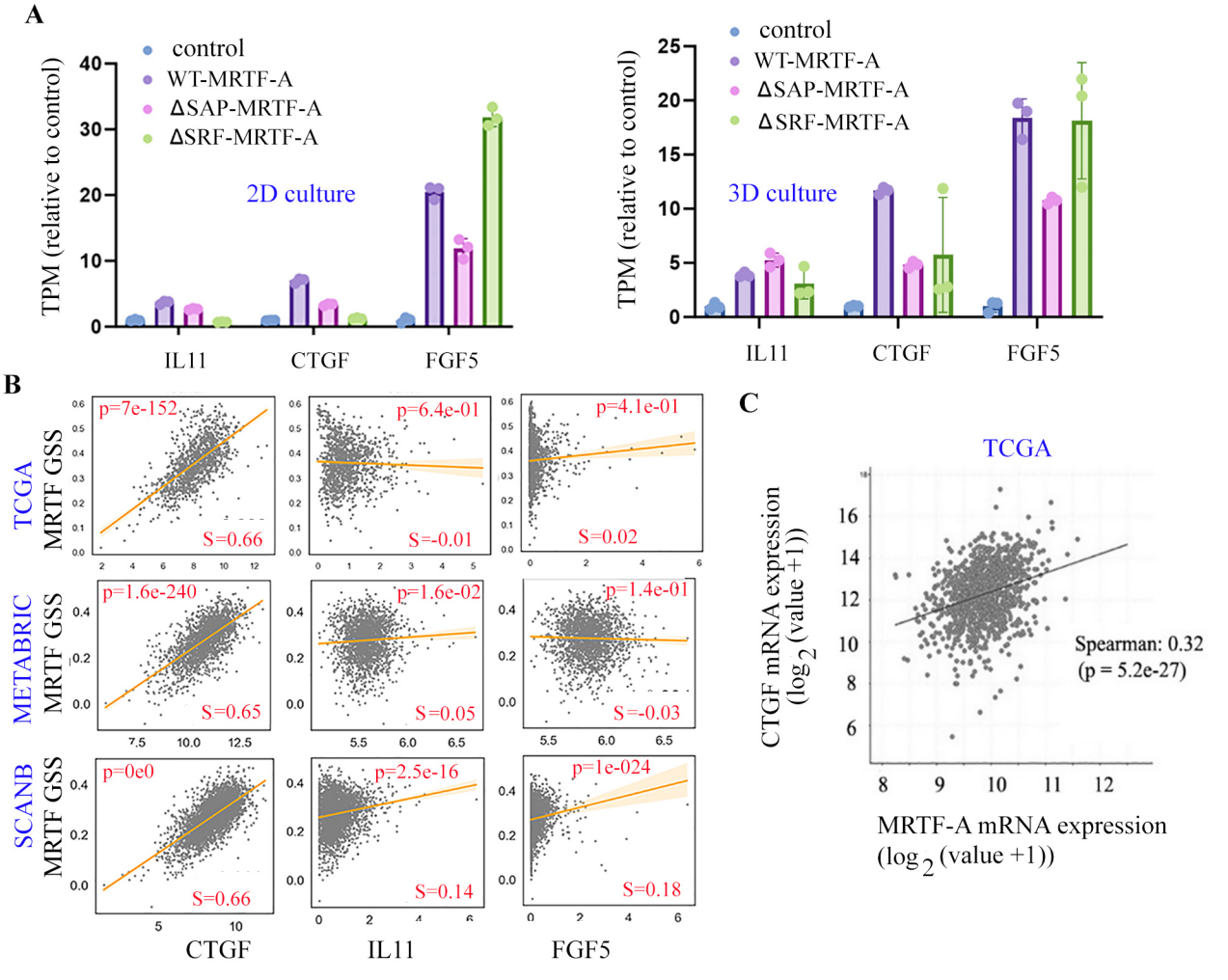

Chawla et al. Figure 5

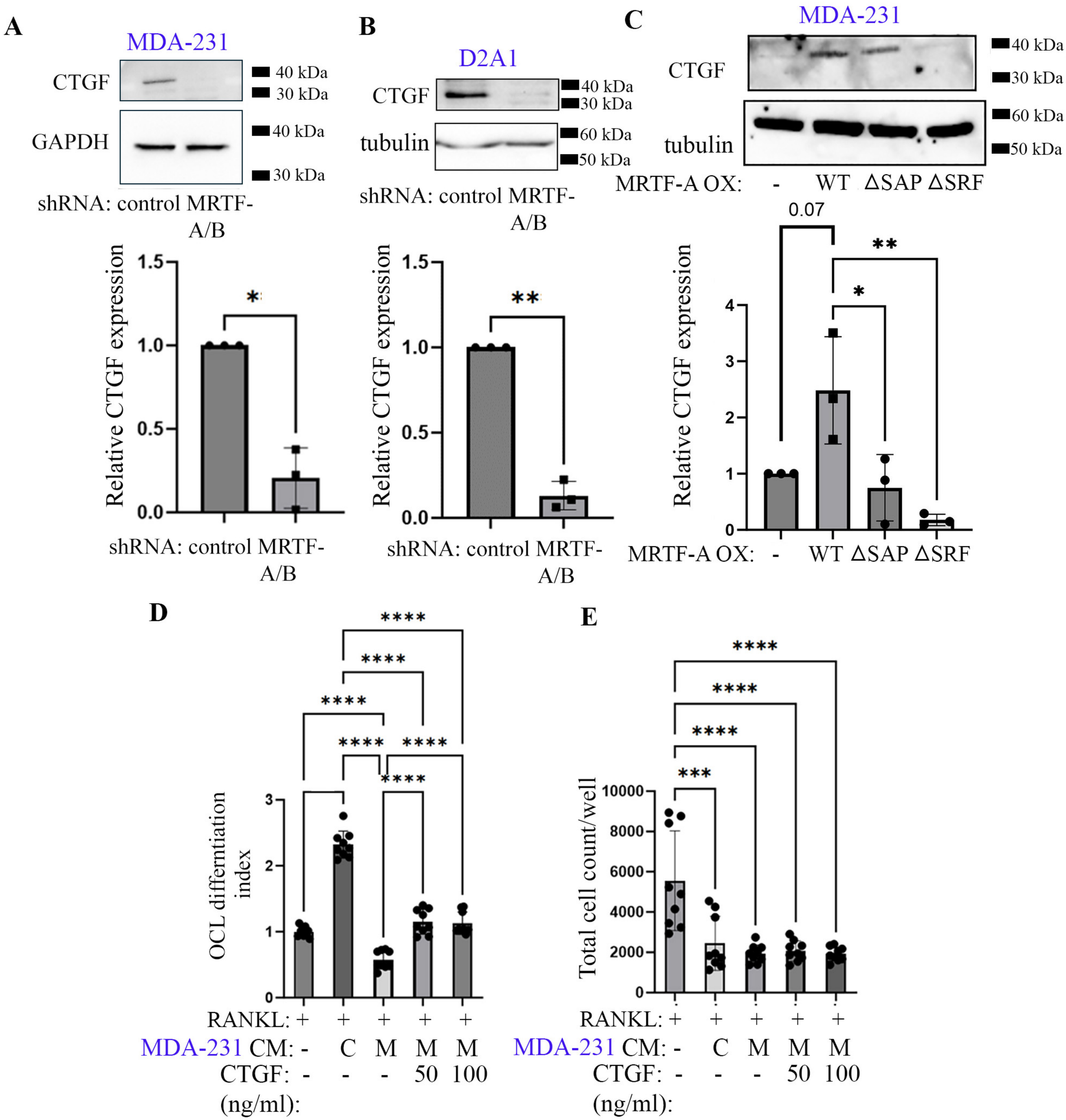

Chawla et al. Figure 6

A

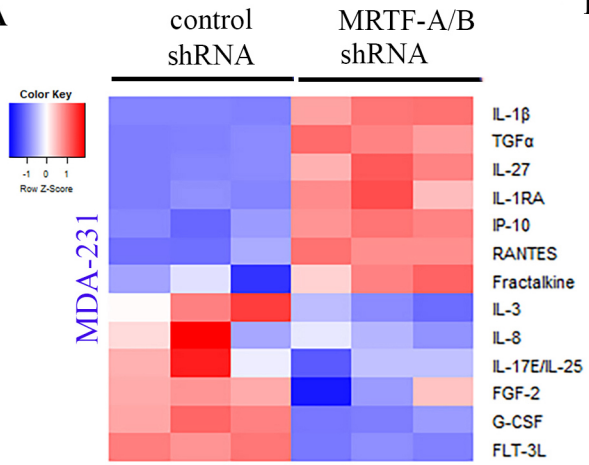

Gene	Fold Change	p-value*
Anti-Osteoclastogenic		
IL-1RA	3.02 ± 0.47	<0.0001
IL-27	6.59 ± 0.99	<0.0001
IL-3	0.39 ± 0.12	0.0475
RANTES	2.11 ± 0.07	<0.0001
Pro-Osteoclastogenic		
FGF-2	0.44 ± 0.45	0.0463
FLT-3L	0.42 ± 0.03	0.0059
Fractalkine	2.63 ± 0.43	<0.0001
G-CSF	0.21 ± 0.06	<0.0001
IL-17E/IL-25	0.31 ± 0.21	<0.0001
IL-1β	3.42 ± 0.27	<0.0001
IL-8	0.58 ± 0.13	0.0053
IP-10	9.54 ± 0.56	<0.0001
TGFα	3.81 ± 0.28	<0.0001

B

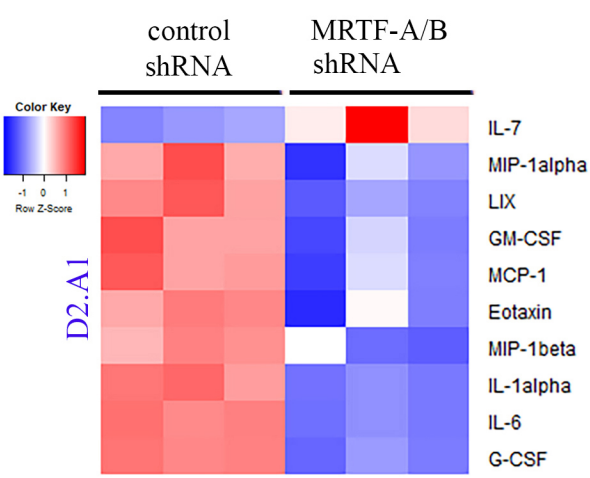

Gene	Fold Change	p-value*
Anti-Osteoclastogenic		
GM-CSF	0.26 ± 0.22	0.0001
LIX	0.24 ± 0.11	<0.0001
Pro-Osteoclastogenic		
Eotaxin	0.44 ± 0.28	0.0005
G-CSF	0.13 ± 0.09	<0.0001
IL-6	0.07 ± 0.06	<0.0001
IL-7	2.99 ± 1.3	<0.0001
MCP-1	0.47 ± 0.18	<0.0001
MIP-1α	0.4 ± 0.23	<0.0001
MIP-1β	0.29 ± 0.25	<0.0001
IL-1α	0.24 ± 0.05	<0.0001

Chawla et al. Figure 7

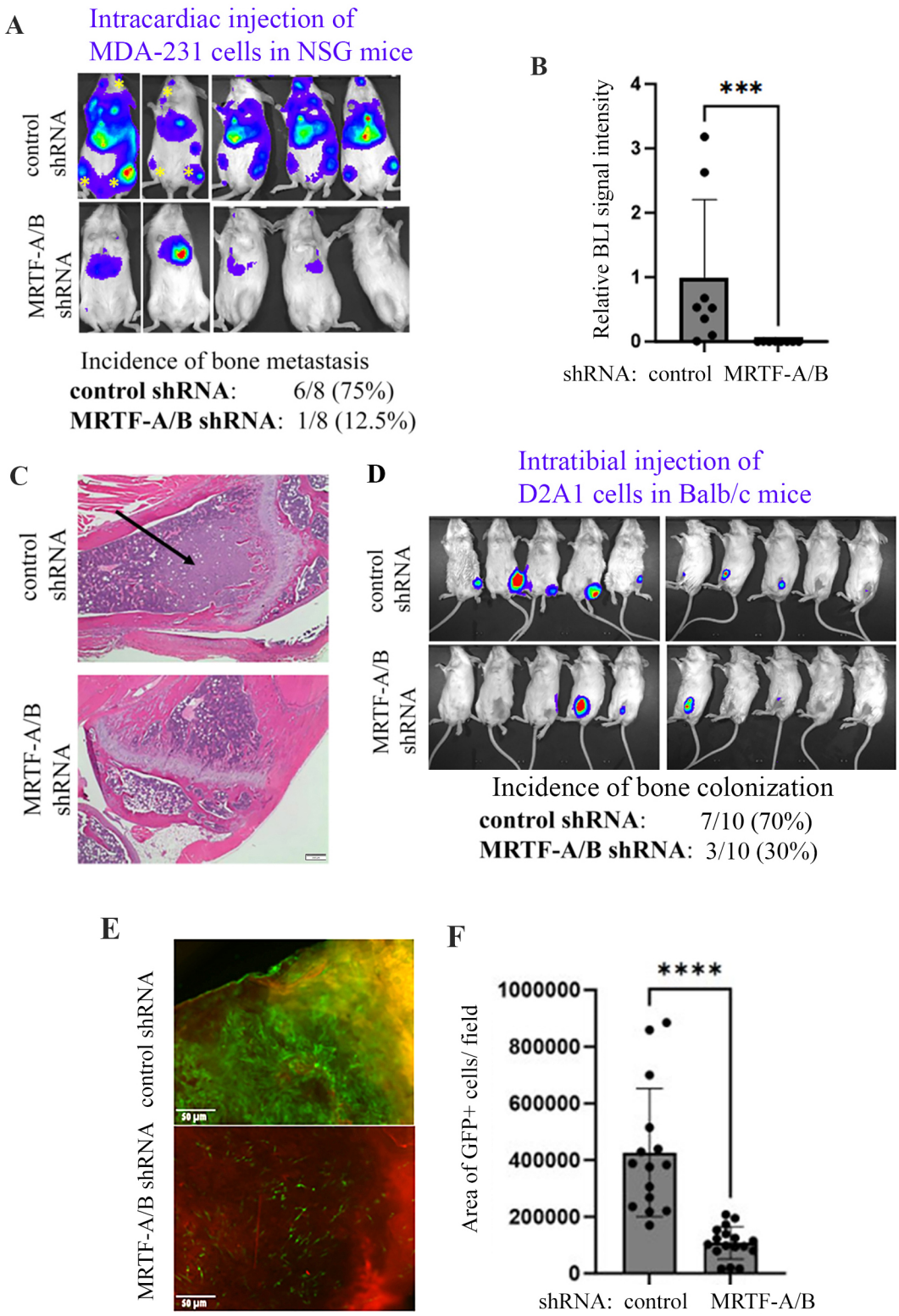

Chawla et al. Figure 8

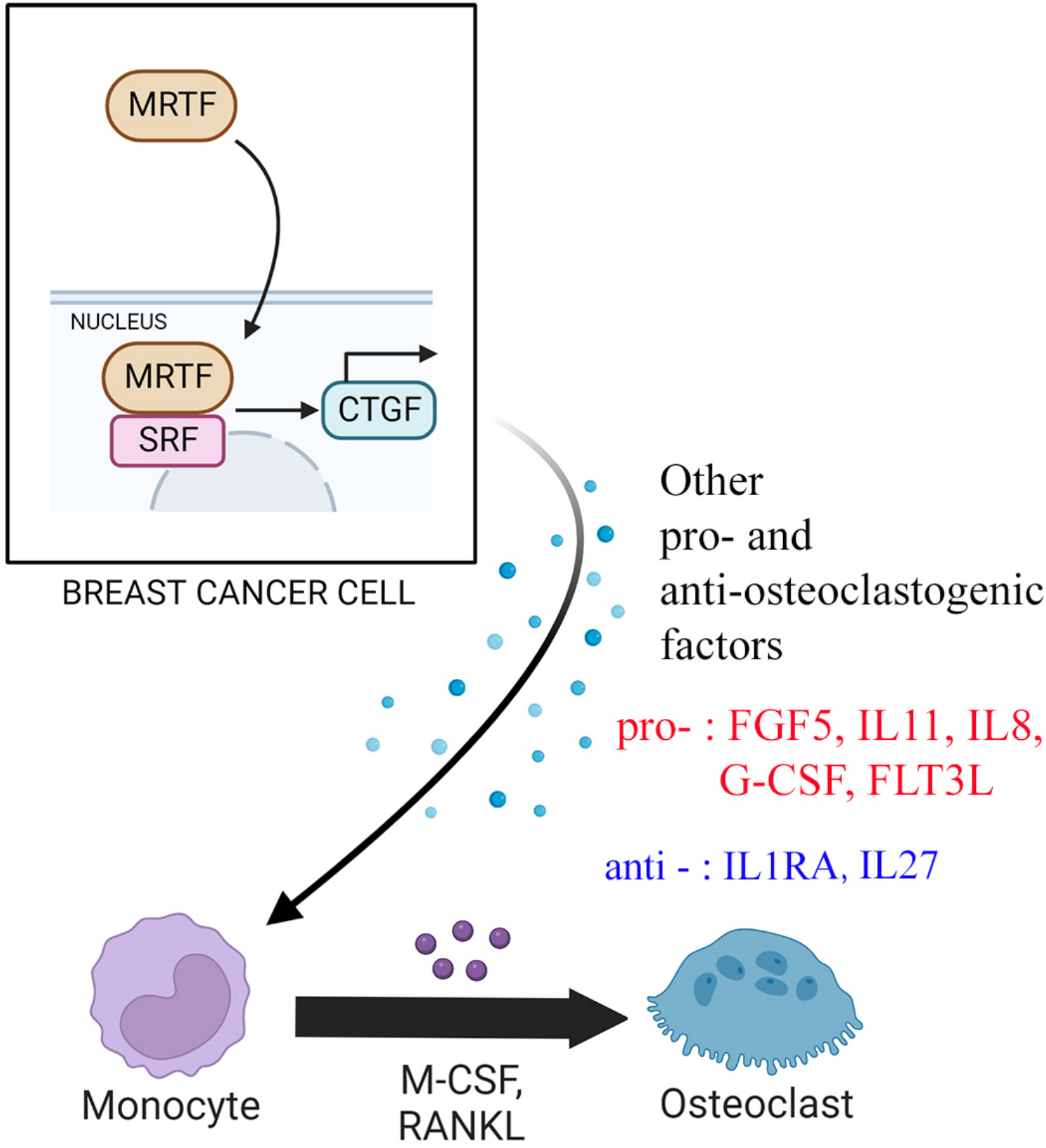

Supporting Information

Breast cancer cells promote osteoclast differentiation in an MRTF-dependent paracrine manner

(Chawla et al.)

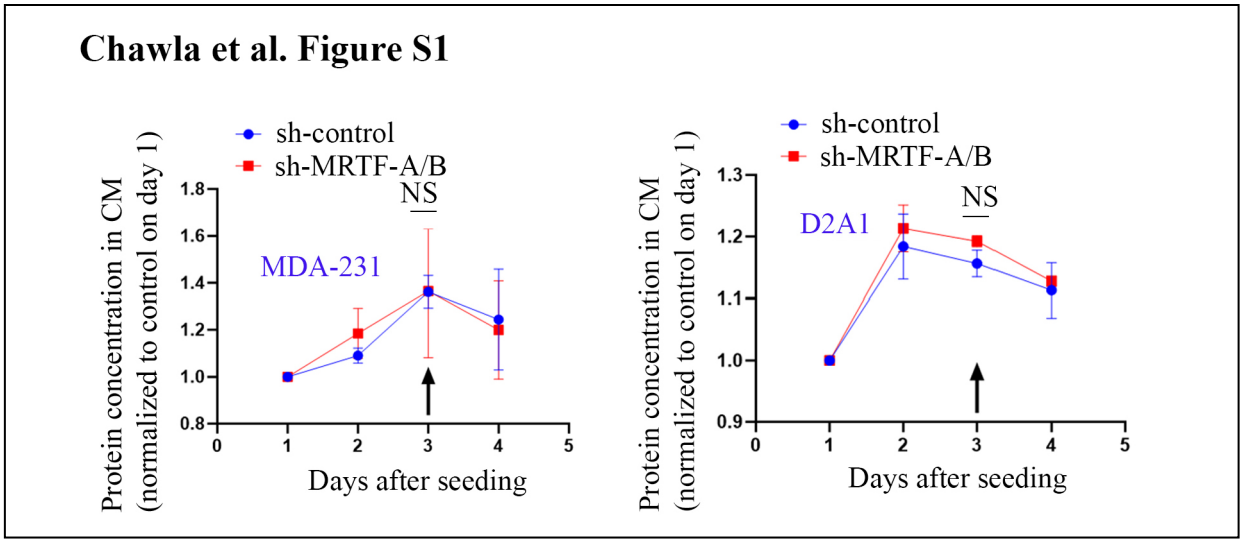

Figure S1: MRTF knockdown does not affect the protein concentration in the CM of breast cancer cells. Protein concentration measured in the CM of control vs stable MRTF-A/B knockdown MDA-231 and D2A1 cells in 2D tissue culture on different days after seeding (data normalized to the value measured for control groups of cells on day 1); arrow indicates the day CM was harvested for OCL differentiation assays).

Chawla et al. Figure S2

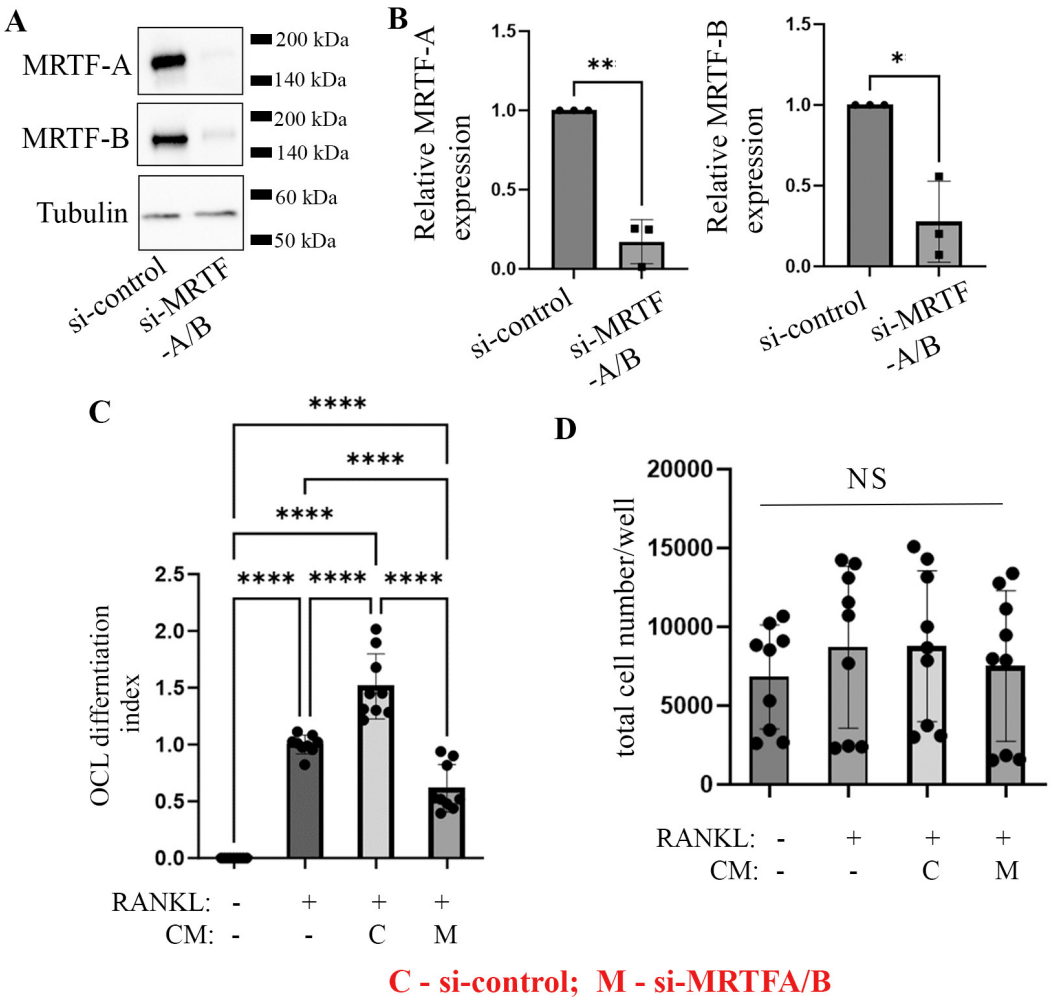

Figure S2: Validation of the effect of MRTF depletion in breast cancer cells on paracrine modulation of OCL differentiation in a transient knockdown setting. A-B) Representative immunoblots (*panel A*) and quantification of immunoblots (*panel B;* data summarized from 3 experiments) of MDA-231 lysates showing siRNA-mediated transient knockdown of MRTF isoforms by siRNAs (isoform-specific MRTF siRNAs were pooled for transfection). **C-D)** Summary of OCL differentiation index (*panel C*) and total cell count (*panel D*) of BMDM cultures subjected to the indicated treatments**;** data summarized from 3 independent experiments (*: $p<0.05$; **: $p<0.01$; ****: $p<0.0001$; NS – not significant).

Supplementary Table S1: Breast cancer bone metastasis gene signature

Direction of change	Genes
Upregulated	*CXCR4, MMP1, ADAMTS1, FGF5, CTGF, IL11, FST, NFAT1, Ph4, and BBS1*
Downregulated	*APOBEc3B, NUP155, MFAP3L, NIP7, C6orf17, KCNS1, STEAP3, C16orf61, PALM2, ATL2, and SFT2D2*

** compiled from Kang, et al. 2003; Savci-Heijink, et al. 2016

Supplementary Table S2: List of cytokines/chemokines analyzed by Luminex assays

Luminex Panel	Cytokines/Chemokines probed
HD-48plex (human)	sCD40L, EGF, Eotaxin, FGF-2, Flt-3 ligand, Fractalkine, G-CSF, GM-CSF, GROα, IFNα2, IFNγ, IL-1α, IL-1β, IL-1ra, IL-2, IL-3, IL-4, IL-5, IL-6, IL-7, IL-8, IL-9, IL-10, IL-12p40, IL-12p70, IL-13, IL-15, IL-17A, IL-17E/IL-25, IL-17F, IL-18, IL-22, IL-27, IP-10, MCP-1, MCP-3, M-CSF, MDC (CCL22), MIG, MIP-1α, MIP-1β, PDGF-AA, PDGF-AB/BB, RANTES, TGFα, TNFα, TNFβ, VEGF-A
MD-32plex (mouse)	Eotaxin, G-CSF, GM-CSF, IFNγ, IL-1α, IL-1β, IL-2, IL-3, IL-4, IL-5, IL-6, IL-7, IL-9, IL-10, IL-12p40, IL-12p70, IL-13, IL-15, IL-17A, IP-10, KC, LIF, LIX, MCP-1, M-CSF, MIG, MIP-1α, MIP-1β, MIP-2, RANTES, TNFα, VEGF-A

Supplementary Table S3: RT-PCR Primer details

Gene name	Primer sequence
Cathepsin-K	5'-GAAGAAGACTCACCAGAAGCAG-3' (sense) 5'-TCCAGGTTATGGGCAGAGATT-3' (antisense).
DC-Stamp	5'-TTGCCGCTGTGGACTATCTG-3' (sense) 5'-GAATGCAGCTCGGTTCAAAC-3' (antisense)